

1 Article

2 **Effect of Geometric Nonlinearity on Aerodynamic**
3 **Stability of Membrane Roofs**4 **Weiju Song¹, Xinxin Wang^{1,*} and Changjiang Liu²**5 ¹ College of Civil Engineering, Hebei University of Engineering, Handan Hebei 056038, China;
6 nimrodsong@126.com(Weiju Song); wangxinxin127@126.com(Xinxin Wang)7 ² School of Civil Engineering, Guangzhou University, Guangzhou, 510006, China; cjliu@gzhu.edu.cn

8 * Correspondence: wangxinxin127@126.com; Tel.: +86-1592-336-3074

9 **Abstract:** Membrane materials are most widely applied in construction engineering with
 10 small mass and high flexibility, it presents strong geometric nonlinearity in the process of
 11 vibration. In the paper, an improved multi-scale perturbation method is used to solve the
 12 aeroelastic stability of closed and open membrane roofs for quantify the effect of geometric
 13 nonlinearity on the single-mode aeroelastic instability wind speed of membrane roofs. The
 14 results show that the critical wind speed values of the two models are small when the
 15 geometrical nonlinearity of membrane material is neglected. In addition, under normal wind
 16 load, the influence of geometrical nonlinearity of membrane on the aerodynamic stability of
 17 roof can be neglected, However, under strong wind load, when the roof deformation reaches
 18 3% of the span, the influence of geometric nonlinearity should be considered and the influence
 19 increases with the decrease of transverse and downwind span of membrane roof. The results
 20 obtained in this paper have important theoretical reference value for the design the membrane
 21 structures.

22 **Keywords:** geometric nonlinearity; improved multiscale method; orthotropic membrane;
 23 aeroelastic instability

25 **1. Introduction**

26 Fabric membrane is the most widely used membrane material in construction engineering. It
 27 has the characteristics of high tensile strength and good flexibility. Fabric membranes are mainly
 28 composed of substrates and coatings. The substrates are usually braided by orthogonal fibers, which
 29 results in the orthotropic properties of the membranes, That is to say, the elastic modulus and
 30 Poisson's ratio in the two orthogonal directions are different. The building which is made up of
 31 membrane material covered on the structure skeleton or tensioned as a whole has beautiful
 32 appearance, good transparency, environmental protection and energy saving [1, 2]. Therefore, it is
 33 widely used in large-scale stadiums, exhibition venues and other public buildings. Because of the
 34 small mass and flexibility , it is easy to vibration under external disturbance. and the stiffness of the
 35 membrane material is small, which results in the large vibration deformation of the membrane
 36 structure under wind load, showing strong geometric non-linearity. Many research results shows
 37 that the single-mode aeroelastic instability can easily occur in membrane structures when the
 38 pre-tension of membrane materials is small [3, 4].

39 In the mathematical analysis of aeroelastic instability of flexible membrane structures, Yang
 40 et al. [5, 6] established the wind-induced dynamic coupling equation of hyperbolic parabolic
 41 membrane roofs with small sag by using elastic shallow shell theory and ideal fluid potential flow
 42 theory in 2006, and determined the critical wind speed of aeroelastic instability according to
 43 Routh-Hurwitz stability criterion. The influence of geometric nonlinearity of membranes was not
 44 taken into account when establishing the mathematical model. In 2011, Zheng et al. [7, 8] studied
 45 the non-linear aerodynamic stability of orthotropic tensioned membrane structures in rectangular

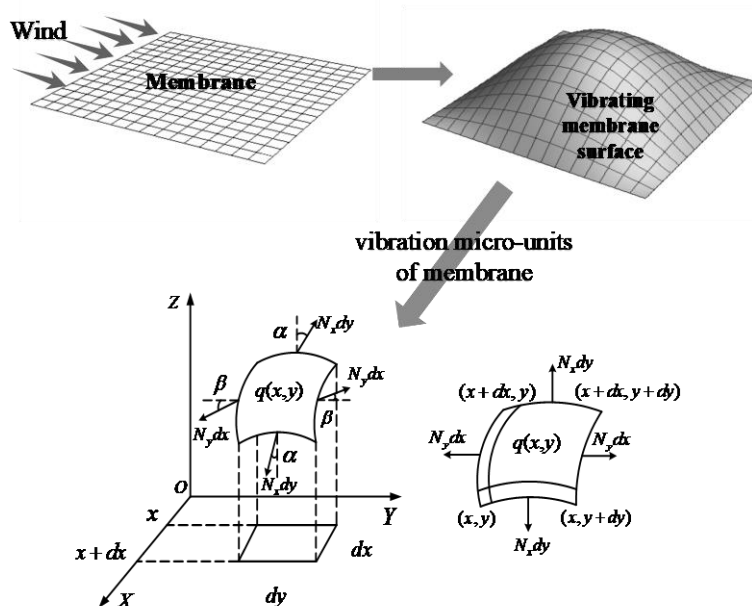
46 plane and hyperbolic paraboloid respectively. The critical wind velocities of single-mode instability
 47 of two membrane structures were determined by assuming the solution of vibration equation. In
 48 2017, Liu et al. [9] studied the aerodynamic stability of closed tensioned membrane structures by
 49 Galerkin method. The geometric nonlinearity of membrane vibration is weakened, and the critical
 50 wind speed of instability is obtained by using the weak nonlinearity solution method.

51 In order to investigate the influence of geometric nonlinearity on the aeroelastic stability of
 52 membrane materials, the nonlinear wind-induced dynamic equations of membrane roofs are
 53 established based on Von Kamen's large deflection theory and Darumbel's principle, taking the flat
 54 rectangular orthotropic tensioned membrane roofs with fixed supports on the four sides of open
 55 and closed structures as analytical models and considering the effects of geometric nonlinearity and
 56 air damping of membrane materials. An improved multi-scale method which suitable for strong
 57 geometric nonlinearity is used to solve the vibration equation. The critical wind speed of instability
 58 obtained is compared with the results without considering geometric nonlinearity. The effect of
 59 geometric nonlinearity on the wind speed of single-mode aeroelastic instability of membrane
 60 material is obtained quantitatively.

61 2. Analytical deduction of single-mode instability of orthotropic membrane aeroelasticity

62 2.1. Establishment of Basic Equations

63 Let the length and width of the orthotropic rectangular flexible membrane with four sides
 64 fixed be a and b respectively; the pre-tension along the length direction is N_{0x} and the width
 65 direction is N_{0y} . The wind blows parallel to the roof and toward the membrane surface, which
 66 makes the membrane surface vibrate. For flexible membranes, the research results show that
 67 the shear stress has little influence on the vibration process of the membranes and can be
 68 considered as zero[10]. Assuming that the planar membrane is in the xoy plane when
 69 equilibrium, and the pre-tension in the x direction is N_x and in the Y direction is N_y , When the
 70 membrane is disturbed by external forces perpendicular to the xoy plane, it will deform and
 71 then produce transverse vibration perpendicular to the membrane surface under the action of
 72 tension. Taking a vibrating micro-units on the vibrating membrane surface as shown in Figure
 73 1.



75 **Figure 1.** Vibration micro-units of membrane

76 Taking the element $dx dy$ on the membrane surface. When the micro-facets are deformed,
 77 the edges of the micro-facets are subjected to the tension of the adjacent facets. In the

78 X-direction, we can regard the surface element as composed of countless chord elements with
 79 length dx and width of one unit. The tension acting on the chord element is consistent with its
 80 tangent direction. The tension N_x is at an angle α with the x coordinate axis. Therefore, the
 81 vertical component of the tension acting on the chord element at one end of X is $N_x \sin \alpha$.
 82 because α is small, $\sin \alpha \approx \tan \alpha$. Let w be the vertical displacement of a point on the membrane
 83 away from the equilibrium position. Therefore:

$$84 \quad N_x \sin \alpha = N_x \tan \alpha = N_x \left(\frac{\partial w}{\partial x} \right)_x \quad (1)$$

85 The vertical force acting on the dy edge is: $N_x \left(\frac{\partial w}{\partial x} \right)_x dy$; and the vertical force at the x
 86 edge should be: $N_x \left(\frac{\partial w}{\partial x} \right)_{x+dx} dy$. Thus, the resultant force in the vertical direction on the x and
 87 $x+dx$ sides of the panel is as follows:

$$88 \quad N_x \left(\frac{\partial w}{\partial x} \right)_{x+dx} dy - N_x \left(\frac{\partial w}{\partial x} \right)_x dy = N_x \frac{\partial^2 w}{\partial x^2} dx dy \quad (2)$$

89 Similarly, the resultant force of the vertical component of the tension acting on the Y
 90 direction can be obtained as follows:

$$91 \quad N_y \left(\frac{\partial w}{\partial y} \right)_{y+dy} dx - N_y \left(\frac{\partial w}{\partial y} \right)_y dx = N_y \frac{\partial^2 w}{\partial y^2} dx dy \quad (3)$$

92 So the total vertical force acting on the whole panel is:

$$93 \quad F_z = N_x \frac{\partial^2 w}{\partial x^2} dx dy + N_y \frac{\partial^2 w}{\partial y^2} dx dy + q(x, y) dx dy \quad (4)$$

94 Where, N_x is the tension in the x direction (longitude), N_y is the tension in the y direction
 95 (latitude), w is the deflection of the membrane, and $q(x, y)$ is the external load acting on the
 96 unit area of the projection surface of the membrane. According to the force balance, we can
 97 obtained that:

$$98 \quad N_x \frac{\partial^2 w}{\partial x^2} dx dy + N_y \frac{\partial^2 w}{\partial y^2} dx dy + q(x, y) dx dy = 0 \quad (5)$$

$$99 \quad q(x, y) + N_x \frac{\partial^2 w}{\partial x^2} + N_y \frac{\partial^2 w}{\partial y^2} = 0 \quad (6)$$

100 The generalized external loads of flexible membrane roof under wind load include the
 101 wind load acting on the membrane surface, structural damping force and inertial force [10]. If
 102 the aerodynamic term is defined as p , then the generalized external load per unit area
 103 $q(x, y)$ is:

$$104 \quad q(x, y) = p(x, y, t) - 2\rho c \frac{\partial w(x, y, t)}{\partial t} - \rho \frac{\partial^2 w(x, y, t)}{\partial t^2} \quad (7)$$

105 For membrane material, the stiffness of membrane surface comes from the initial
 106 pre-tension of membrane material, so the initial pre-tension should be added in formula 6.
 107 Finally, the differential equations of motion of flexible membranes are obtained as follows:

108
$$p(x, y, t) - 2\rho c \frac{\partial w(x, y, t)}{\partial t} - \rho \frac{\partial^2 w(x, y, t)}{\partial t^2} + (N_{0x} + N_{xt}) \frac{\partial^2 w}{\partial x^2} + (N_{0y} + N_{yt}) \frac{\partial^2 w}{\partial y^2} = 0 \quad (8)$$

109 Introducing the stress function $\varphi(x, y)$, $N_x = h \frac{\partial^2 \varphi}{\partial y^2}$, $N_y = h \frac{\partial^2 \varphi}{\partial x^2}$, Then equation (6)
 110 becomes:

111
$$\left(N_{0x} + h \frac{\partial^2 \varphi}{\partial y^2} \right) \frac{\partial^2 w}{\partial x^2} + \left(N_{0y} + h \frac{\partial^2 \varphi}{\partial x^2} \right) \frac{\partial^2 w}{\partial y^2} + p - 2\rho c \frac{\partial w}{\partial t} - \rho \frac{\partial^2 w}{\partial t^2} = 0 \quad (9)$$

112 After deformation, the membrane surface strain is composed of linear and non-linear parts.
 113 The linear strain is caused by in-plane displacement u and v , and the non-linear strain is
 114 caused by deflection w . After ignoring shear stress, the total strain is as follows:

115
$$\left. \begin{aligned} \varepsilon_x &= \frac{\partial u}{\partial x} + \frac{1}{2} \left(\frac{\partial w}{\partial x} \right)^2 \\ \varepsilon_y &= \frac{\partial v}{\partial y} + \frac{1}{2} \left(\frac{\partial w}{\partial y} \right)^2 \end{aligned} \right\} \quad (10)$$

116 Where, ε_x is the strain in the X direction, ε_y is the strain in the Y direction.

117 By eliminating u and v in equation (10), the continuous deformation conditions satisfying
 118 the strain and deflection of the film surface can be obtained.

119
$$\frac{\partial^2 \varepsilon_x}{\partial y^2} + \frac{\partial^2 \varepsilon_y}{\partial x^2} = \left(\frac{\partial^2 w}{\partial x \partial y} \right)^2 - \frac{\partial^2 w}{\partial x^2} \frac{\partial^2 w}{\partial y^2} \quad (11)$$

120 The membrane is orthotropic, and the direction of the fiber is the main direction of
 121 elasticity, so that it is consistent with the direction of coordinate system X and Y. Assuming
 122 that the direction of fiber is the same as the direction of coordinate system X and Y. The
 123 Young's modulus of elasticity in X and Y directions is E_1 and E_2 , respectively. The longitudinal
 124 Poisson's ratio and the latitudinal Poisson's ratio is μ_1 and μ_2 , respectively. The relationship
 125 between elastic modulus and Poisson's ratio is as follows.

126
$$\frac{\mu_1}{E_1} = \frac{\mu_2}{E_2} \quad (12)$$

127 The stress-strain relationship is as follows:

128
$$\begin{Bmatrix} \sigma_x \\ \sigma_y \end{Bmatrix} = \begin{Bmatrix} \frac{E_1}{1 - \mu_1 \mu_2} & \frac{\mu_1 E_2}{1 - \mu_1 \mu_2} \\ \frac{\mu_2 E_1}{1 - \mu_1 \mu_2} & \frac{E_2}{1 - \mu_1 \mu_2} \end{Bmatrix} \begin{Bmatrix} \varepsilon_x \\ \varepsilon_y \end{Bmatrix} \quad (13)$$

129 Where σ_x and σ_y is the normal stresses in the X direction and Y direction respectively. h is
 130 the thickness of membrane.

131 Letting $N_x = h \cdot \sigma_x$, $N_y = h \cdot \sigma_y$, substituting Equation (13) into Equation (11), the
 132 compatibility equation is obtained as follows:

$$\begin{aligned}
 133 \quad & \frac{1}{E_1 h} \frac{\partial^2 N_x}{\partial y^2} - \frac{\mu_2}{E_2 h} \frac{\partial^2 N_y}{\partial y^2} - \frac{\mu_1}{E_1 h} \frac{\partial^2 N_x}{\partial x^2} + \frac{1}{E_2 h} \frac{\partial^2 N_y}{\partial x^2} \\
 & = \left(\frac{\partial^2 w}{\partial x \partial y} \right)^2 - \frac{\partial^2 w}{\partial x^2} \frac{\partial^2 w}{\partial y^2}
 \end{aligned} \tag{14}$$

134 By substituting the stress function into Equation (14), it can be transformed into:

$$\begin{aligned}
 135 \quad & \frac{1}{E_1} \frac{\partial^4 \varphi}{\partial y^4} - \frac{\mu_2}{E_2} \frac{\partial^4 \varphi}{\partial x^2 \partial y^2} - \frac{\mu_1}{E_1} \frac{\partial^4 \varphi}{\partial x^2 \partial y^2} + \frac{1}{E_2} \frac{\partial^4 \varphi}{\partial x^4} \\
 & = \left(\frac{\partial^2 w}{\partial x \partial y} \right)^2 - \frac{\partial^2 w}{\partial x^2} \frac{\partial^2 w}{\partial y^2}
 \end{aligned} \tag{15}$$

136 2.2. Modified multiscale solutions of governing equations

137 The initial surface function of rectangular planar membrane $z_0(x, y) = 0$, then the surface
138 equation of flexible membrane under wind load is as follows:

$$139 \quad z(x, y, t) = w(x, y, t) \tag{16}$$

140 According to the Bubnov-Galerkin method, assuming the solution of the governing equation
141 is [9, 10].

$$\begin{aligned}
 142 \quad & \begin{cases} w(x, y, t) = \sum_{i=1}^n T_i(t) W_i(x, y) \\ \varphi(x, y, t) = \sum_{i=1}^n U_i(t) \phi_i(x, y) \end{cases} \tag{17}
 \end{aligned}$$

143 Where $W_i(x, y)$ is the mode function, $\phi_i(x, y)$ is the unknown stress function about the
144 coordinates, $T_i(t)$ and $U_i(t)$ are the time-dependent function.
145

146 Because the membrane is fixed on four sides, the vertical deflection at the boundary of the
membrane is zero, and the vibration mode function satisfying the conditions is assumed to be:

$$147 \quad W(x, y) = \sin \frac{m\pi x}{a} \sin \frac{n\pi y}{b} \tag{18}$$

148 where m and n are positive integer, which denote sinusoidal half wave number.

149 substituting Equation (18) into Equation (17), the following equation is obtained:

$$150 \quad w(x, y, t) = T(t) \sin \frac{m\pi x}{a} \sin \frac{n\pi y}{b} \tag{19}$$

151 Substituting Equation (19) into Equation (15), yields:

$$152 \quad \frac{1}{E_1} \frac{\partial^4 \varphi}{\partial y^4} + \frac{1}{E_2} \frac{\partial^4 \varphi}{\partial x^4} = \frac{m^2 n^2 \pi^4}{2a^2 b^2} T^2(t) \left(\cos \frac{2m\pi x}{a} + \cos \frac{2n\pi y}{b} \right) \tag{20}$$

153 Assuming that the solution of stress function in formula (20) is

$$\begin{aligned}
 154 \quad & \begin{cases} \varphi(x, y, t) = T^2(t) \phi(x, y) \\ \phi(x, y) = \alpha \cos \frac{2m\pi x}{a} + \beta \cos \frac{2n\pi y}{b} \end{cases} \tag{21}
 \end{aligned}$$

155 substituting Equation (21) into Equation (20), yields:

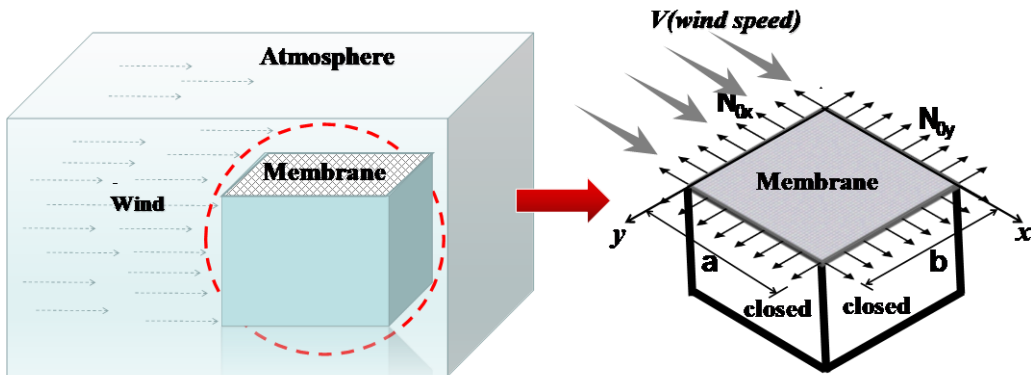
156

157

$$\alpha = \frac{E_2 a^2 n^2}{32 b^2 m^2}, \quad \beta = \frac{E_1 b^2 m^2}{32 a^2 n^2} \quad (22)$$

158 2.1.1. Solution of Flexible Membrane Roof on Closed Structure

159
160 Flexible membrane covers the top of closed structure as roof, and rigid wall around the
161 structure as vertical bearing member. Because its stiffness is far greater than the membrane's
162 stiffness, it is assumed that the stiffness of vertical component is infinite in the process of
163 theoretical derivation in this paper. The membrane roof on closed structure is shown in Figure
2.



164
165 **Figure 2.** The membrane roof on closed structure

166 For the membrane roof on closed structure, the aerodynamic force acting on the unit area
167 of the membrane projection surface is expressed as follows[8]:

168

$$p = -\frac{\rho_0}{2\pi} \left(-V \iint_{Ra} \frac{\left(V \frac{\partial w}{\partial x} + \frac{\partial w}{\partial t} \right)_{x=\xi} (x-\xi)}{\sqrt{(x-\xi)^2 + (y-\eta)^2}} d\xi d\eta + \iint_{Ra} \frac{\left(V \frac{\partial^2 w}{\partial x \partial t} + \frac{\partial^2 w}{\partial t^2} \right)_{x=\xi} (y-\eta)}{\sqrt{(x-\xi)^2 + (y-\eta)^2}} d\xi d\eta \right) \quad (23)$$

169

Substituting Equation (23) into Equation (9), yields:

170

$$\begin{aligned} & (h \frac{\partial^2 \varphi}{\partial y^2} + N_{0x}) \frac{\partial^2 w}{\partial x^2} + (h \frac{\partial^2 \varphi}{\partial x^2} + N_{0y}) \frac{\partial^2 w}{\partial y^2} - 2\rho c \frac{\partial w}{\partial t} \\ & - \rho \frac{\partial^2 w}{\partial t^2} - \frac{\rho_0}{\pi} \iint_{Ra} \frac{1}{r} \left(\frac{\partial^2 w}{\partial t^2} \right)_{x=\xi} d\xi d\eta - \frac{\rho_0 V}{2\pi} \iint_{Ra} \frac{1}{r} \left(\frac{\partial^2 w}{\partial x \partial t} \right)_{x=\xi} d\xi d\eta \\ & + \frac{\rho_0 V^2}{2\pi} \iint_{Ra} \frac{1}{r^3} \left(\frac{\partial w}{\partial x} \right)_{x=\xi} (x-\xi) d\xi d\eta + \frac{\rho_0 V}{2\pi} \iint_{Ra} \frac{1}{r^3} \left(\frac{\partial w}{\partial t} \right)_{x=\xi} (x-\xi) d\xi d\eta = 0 \end{aligned} \quad (24)$$

171 Where $r = \sqrt{(x-\xi)^2 + (y-\eta)^2}$, the integral region $Ra \in \{0 \leq \xi \leq a, 0 \leq \eta \leq b\}$.

172 Substituting Equations (19), (21) and (22) into Equation (24), yields:

173

$$\begin{aligned} & \left(\rho W + \frac{\rho_0}{\pi} \gamma_1 \right) \frac{d^2 T(t)}{dt^2} + \left[\frac{\rho_0 V}{2\pi} (\gamma_2 - \gamma_4) + 2\rho c W \right] \frac{dT(t)}{dt} \\ & - \left(N_{0x} \frac{\partial^2 W}{\partial x^2} + N_{0y} \frac{\partial^2 W}{\partial y^2} + \frac{\rho_0 V^2}{2\pi} \gamma_3 \right) T(t) - h \left(\frac{\partial^2 \Phi}{\partial y^2} \frac{\partial^2 W}{\partial x^2} + \frac{\partial^2 \Phi}{\partial x^2} \frac{\partial^2 W}{\partial y^2} \right) T^3(t) = 0 \end{aligned} \quad (25)$$

174

Where:

$$\begin{aligned}
 \gamma_1 &= \iint_{Ra} \frac{1}{r} (W)_{\substack{x=\xi \\ y=\eta}} d\xi d\eta = \iint_{Ra} \frac{1}{r} \sin \frac{m\pi\xi}{a} \sin \frac{n\pi\eta}{b} d\xi d\eta \\
 \gamma_2 &= \iint_{Ra} \frac{1}{r} \left(\frac{\partial W}{\partial x} \right)_{\substack{x=\xi \\ y=\eta}} d\xi d\eta = \frac{m\pi}{a} \iint_{Ra} \frac{1}{r} \cos \frac{m\pi\xi}{a} \sin \frac{n\pi\eta}{b} d\xi d\eta \\
 \gamma_3 &= \iint_{Ra} \frac{1}{r^3} \left(\frac{\partial W}{\partial x} \right)_{\substack{x=\xi \\ y=\eta}} (x - \xi) d\xi d\eta = \frac{m\pi}{a} \iint_{Ra} \frac{1}{r^3} (x - \xi) \cos \frac{m\pi\xi}{a} \sin \frac{n\pi\eta}{b} d\xi d\eta \\
 \gamma_4 &= \iint_{Ra} \frac{1}{r^3} (W)_{\substack{x=\xi \\ y=\eta}} (x - \xi) d\xi d\eta = \iint_{Ra} \frac{1}{r^3} (x - \xi) \sin \frac{m\pi\xi}{a} \sin \frac{n\pi\eta}{b} d\xi d\eta
 \end{aligned}$$

175

176

Using Bubnov-Galerkin method to integral Equation (25), yields:

$$\iint_S \left\{ \left(\rho W + \frac{\rho_0}{\pi} \gamma_1 \right) \frac{d^2 T(t)}{dt^2} + \left[\frac{\rho_0 V}{2\pi} (\gamma_2 - \gamma_4) + 2\rho c W \right] \frac{dT(t)}{dt} \right. \\
 \left. - \left(N_{0x} \frac{\partial^2 W}{\partial x^2} + N_{0y} \frac{\partial^2 W}{\partial y^2} + \frac{\rho_0 V^2}{2\pi} \gamma_3 \right) T(t) - h \left(\frac{\partial^2 \Phi}{\partial y^2} \frac{\partial^2 W}{\partial x^2} + \frac{\partial^2 \Phi}{\partial x^2} \frac{\partial^2 W}{\partial y^2} \right) T^3(t) \right\} W(x, y) dx dy = 0 \quad (26)$$

178

179

Where $S \in \{0 \leq x \leq a, 0 \leq y \leq b\}$.

Simplifying Formula (26), yields:

$$A \frac{d^2 T(t)}{dt^2} + B \frac{dT(t)}{dt} - CT(t) - DT^3(t) = 0 \quad (27)$$

181

Where:

$$\begin{aligned}
 A &= \iint_S \left(\rho W + \frac{\rho_0}{\pi} \gamma_1 \right) W dx dy \\
 &= \rho \iint_S \left(\sin \frac{m\pi x}{a} \sin \frac{n\pi y}{b} \right)^2 dx dy + \frac{\rho_0}{\pi} \iint_{Ra} \left(\iint_{Ra} \frac{1}{r} \sin \frac{m\pi\xi}{a} \sin \frac{n\pi\eta}{b} d\xi d\eta \right) \sin \frac{m\pi x}{a} \sin \frac{n\pi y}{b} dx dy \\
 &= \frac{\rho ab}{4} + \frac{\rho_0}{\pi} \alpha_1 \\
 \alpha_1 &= \iint_S \left(\iint_{Ra} \frac{1}{r} \sin \frac{m\pi\xi}{a} \sin \frac{n\pi\eta}{b} d\xi d\eta \right) \sin \frac{m\pi x}{a} \sin \frac{n\pi y}{b} dx dy \\
 B &= \frac{\rho_0 V}{2\pi} \iint_S (\gamma_2 - \gamma_4) W dx dy + 2\rho c \iint_S W^2 dx dy \\
 &= \frac{\rho_0 m V}{2a} \iint_S \left(\iint_{Ra} \frac{1}{r} \cos \frac{m\pi\xi}{a} \sin \frac{n\pi\eta}{b} d\xi d\eta \right) \sin \frac{m\pi x}{a} \sin \frac{n\pi y}{b} dx dy \\
 &\quad - \frac{\rho_0 V}{2\pi} \iint_S \left[\iint_{Ra} \frac{1}{r^3} (x - \xi) \sin \frac{m\pi\xi}{a} \sin \frac{n\pi\eta}{b} d\xi d\eta \right] \sin \frac{m\pi x}{a} \sin \frac{n\pi y}{b} dx dy \\
 &\quad + 2\rho c \iint_S \left(\sin \frac{m\pi x}{a} \sin \frac{n\pi y}{b} \right)^2 dx dy \\
 &= \frac{\rho_0 m V}{2a} \alpha_2 - \frac{\rho_0 V}{2\pi} \alpha_4 + \frac{\rho c ab}{2}
 \end{aligned}$$

183

184
$$\alpha_2 = \iint_S \left(\iint_{Ra} \frac{1}{r} \cos \frac{m\pi\xi}{a} \sin \frac{n\pi\eta}{b} d\xi d\eta \right) \sin \frac{m\pi x}{a} \sin \frac{n\pi y}{b} dx dy$$

$$\alpha_4 = \iint_S \left[\iint_{Ra} \frac{1}{r^3} (x - \xi) \sin \frac{m\pi\xi}{a} \sin \frac{n\pi\eta}{b} d\xi d\eta \right] \sin \frac{m\pi x}{a} \sin \frac{n\pi y}{b} dx dy$$

$$C = \iint_S \left(N_{0x} \frac{\partial^2 W}{\partial x^2} + N_{0y} \frac{\partial^2 W}{\partial y^2} + \frac{\rho_0 V^2}{2\pi} \gamma_3 \right) W dx dy$$

185
$$= \iint_S N_{0x} \frac{\partial^2 W}{\partial x^2} W dx dy + \iint_{Ra} N_{0y} \frac{\partial^2 W}{\partial y^2} W dx dy + \frac{\rho_0 V^2}{2\pi} \iint_{Ra} \gamma_3 W dx dy$$

$$= -\frac{m^2 \pi^2 b N_{0x}}{4a} - \frac{n^2 \pi^2 a N_{0y}}{4b} + \frac{\rho_0 m V^2}{2a} \alpha_3$$

186
$$\alpha_3 = \iint_S \left(\iint_{Ra} \frac{1}{r^3} (x - \xi) \cos \frac{m\pi\xi}{a} \sin \frac{n\pi\eta}{b} d\xi d\eta \right) \sin \frac{m\pi x}{a} \sin \frac{n\pi y}{b} dx dy$$

187
$$D = \iint_S h \left(\frac{\partial^2 \Phi}{\partial y^2} \frac{\partial^2 W}{\partial x^2} + \frac{\partial^2 \Phi}{\partial x^2} \frac{\partial^2 W}{\partial y^2} \right) W dx dy$$

$$= -\frac{h m^2 n^2 \pi^4 (\alpha + \beta)}{2ab}$$

188 It can be obtained from numerical calculation that only when $b/a \ll 0.1$, $A \leq 0$; this will
 189 not happen in practical engineering. Letting $u = B/(\varepsilon A)$, $\omega_0^2 = -C/A$, $\varepsilon = -D/A$. Then the
 190 equation (27) is transformed into:

191
$$\ddot{T} + \omega_0^2 T + \varepsilon \left(\mu \dot{T} + T^3 \right) = 0 \quad (28)$$

192 Letting ω is the vibration frequency of membrane material and expanding ω^2 to the
 193 power series of ε near ω_0^2 as follows:

194
$$\omega^2 = \omega_0^2 + \varepsilon \omega_1 + \varepsilon^2 \omega_2 + \dots \quad (29)$$

195 The transformation parameters are introduced as follows.

196
$$\alpha = \frac{\varepsilon \omega_1}{\omega_0^2 + \varepsilon \omega_1} \quad (30)$$

197
$$\varepsilon = \frac{\omega_0^2 \alpha}{\omega_1 (1 - \alpha)} \quad (31)$$

198
$$\omega_0^2 + \varepsilon \omega_1 = \frac{\omega_0^2}{1 - \alpha}$$

199 Expanding ω^2 to the power series of ε as follows:

200
$$\omega^2 = \omega_0^2 + \varepsilon \omega_1 \left[1 + \frac{1}{\omega_0^2 + \varepsilon \omega_1} (\varepsilon^2 \omega_2 + \varepsilon^3 \omega_3 + \dots) \right] = \frac{\omega_0^2}{1 - \alpha} (1 + \delta_2 \alpha^2 + \delta_3 \alpha^3 + \dots) \quad (32)$$

201
$$\omega = \omega_0 \left[1 + \frac{1}{2} \alpha + \left(\frac{3}{8} + \frac{\delta^2}{2} \right) \alpha^2 + \dots \right] \quad (33)$$

202 The form of perturbation solution of the equation (28) can be:

203
$$T(t, \alpha) = T_0(t_0, t_1) + \alpha T_1(t_0, t_1) + \alpha^2 T_2(t_0, t_1) + \dots \quad (34)$$

204 Where $t_0 = t$, $t_1 = \alpha t$.

205 The differential operators are obtained as follows.

205

$$\frac{d}{dt} = D_0 + \alpha D_1 + \alpha^2 D_2 + \dots, \quad (35)$$

$$\frac{d^2}{dt^2} = D_0^2 + 2\alpha D_0 D_1 + \alpha^2 (D_1^2 + 2D_0 D_2) + \dots$$

206

Substituting Equations (30), (31), (32) and (34) into Equation (28), yields:

207

$$(1-\alpha) \left[D_0^2 + 2\alpha D_0 D_1 + \alpha^2 (D_1^2 + 2D_0 D_2) \right] (T_0 + \alpha T_1 + \alpha^2 T_2 + \dots) \\ + (1-\alpha) \omega_0^2 (T_0 + \alpha T_1 + \alpha^2 T_2 + \dots) + \frac{\alpha \omega_0^2}{\omega_1^2} \left[(T_0 + \alpha T_1 + \alpha^2 T_2 + \dots)^3 + (D_0 + \alpha D_1 + \alpha^2 D_2) \cdot \right. \\ \left. (T_0 + \alpha T_1 + \alpha^2 T_2 + \dots) \right] \\ = 0$$

208

(36)

209

$$\alpha^0 \quad D_0^2 T_0 + \omega_0^2 T_0 = 0$$

$$\alpha^1 \quad D_0^2 T_1 + \omega_0^2 T_1 + 2D_0 D_1 T_0 + \frac{\omega_0^2}{\omega_1} (D_0 T_0 + T_0^3) = 0 \quad (37)$$

$$\alpha^2 \quad D_0^2 T_2 + T_2 + 2D_0 D_1 T_1 + (D_1^2 + 2D_0 D_2) T_0 + \frac{\omega_0^2}{\omega_1} 3T_0^2 T_1 = 0$$

210

The solution of the first equation in the system of equations (37) can be as follows:

211

212

$$T_0 = A(t_1) e^{i\omega_0 t_0} + \bar{A}(t_1) e^{-i\omega_0 t_0} \quad (38)$$

Substituting Equation (38) into The Second Equation in Equation (37), yields:

213

214

$$D_0^2 T_1 + \omega_0^2 T_1 + \left(2i\omega_0 D_1 A + 3 \frac{\omega_0^2}{\omega_1} A^2 \bar{A} + i\mu \frac{\omega_0^3}{\omega_1} A \right) e^{i t_0} + \frac{1}{\omega_1} A^3 e^{3 i t_0} + cc = 0 \quad (39)$$

215

Where cc is the conjugate complex term. Eliminating the term of immortality in equation (39), yields:

216

217

$$2D_1 A + 3 \frac{\omega_0}{\omega_1} A^2 \bar{A} + i\mu \frac{\omega_0^3}{\omega_1} A = 0 \quad (40)$$

Solving equation (40), we can obtain:

218

$$T_1 = \frac{1}{8\omega_1} (A^3 e^{3 i t_0} + \bar{A}^3 e^{-3 i t_0}) \quad (41)$$

219

Letting $A = \frac{1}{2} f e^{i\phi}$, bring it into equation (41) and separating the imaginary part from the real part.

220

221

$$\frac{df}{dt_1} = -\frac{1}{2} \mu \frac{\omega_0^2}{\omega_1} f, \quad f \frac{d\phi}{dt_1} = -\frac{3\omega_0}{8\omega_1} f^3 \quad (42)$$

222

Substituting $A = \frac{1}{2} f e^{i\phi}$ into Equation (38), yields:

223

224

$$T_0 = f \cos(\omega_0 t_0 + \phi) = f \cos(\omega t + \phi_0) \quad (43)$$

225

Comparing the angular frequency in equation (33) with equation (43), we can get the equation under the first order approximation condition as follows.

226

227

$$\frac{d\phi}{dt_1} = \frac{\omega_0}{2} \quad (44)$$

According to the equations (42) and (43), yields:

228

$$\omega_1 = \frac{3}{4} f^2 \quad (45)$$

229

Substituting Equation (45) into Equation (42) and omitting higher order terms, yields:

230

$$\omega = \sqrt{\omega_0^2 + \frac{3}{4}\varepsilon f^2} \quad (46)$$

231

The results show that when the critical wind speed of single mode instability is reached, the frequency of the characteristic equation of the system approaches zero, which is equivalent to static equilibrium instability [9]. That is:

234

$$\omega_0^2 + \frac{3}{4}\varepsilon f^2 = 0 \quad (47)$$

235

Where f is the vibration amplitude of membrane,

236

$$\omega_0^2 = \frac{2\pi}{\rho ab\pi + 4\rho_0\alpha_1} \cdot \left(\frac{m^2\pi^2b^2N_{0x} + n^2\pi^2a^2N_{0y}}{2ab} - \frac{\rho_0 m \alpha_3}{a} V^2 \right)$$

$$\alpha_1 = \iint_S \left(\iint_{Ra} \frac{1}{r} \sin \frac{m\pi\xi}{a} \sin \frac{n\pi\eta}{b} d\xi d\eta \right) \sin \frac{m\pi x}{a} \sin \frac{n\pi y}{b} dx dy$$

$$\alpha_3 = \iint_S \left(\iint_{Ra} \frac{1}{r^3} (x - \xi) \cos \frac{m\pi\xi}{a} \sin \frac{n\pi\eta}{b} d\xi d\eta \right) \sin \frac{m\pi x}{a} \sin \frac{n\pi y}{b} dx dy$$

237

$$\varepsilon = \frac{2hm^2n^2\pi^5(\alpha + \beta)}{ab(\rho ab\pi + 4\rho_0\alpha_1)}$$

238

Solving the equation, the critical wind speed for single mode instability of closed membrane roof is obtained as follows:

240

$$V_{cr} = \sqrt{\frac{4\pi(m^2\pi^2b^2N_{0x} + n^2\pi^2a^2N_{0y}) + 3\varepsilon f^2(\rho\pi a^2b^2 + 4\rho_0 ab\alpha_1)}{8\pi b\rho_0 m \alpha_3}} \quad (48)$$

241

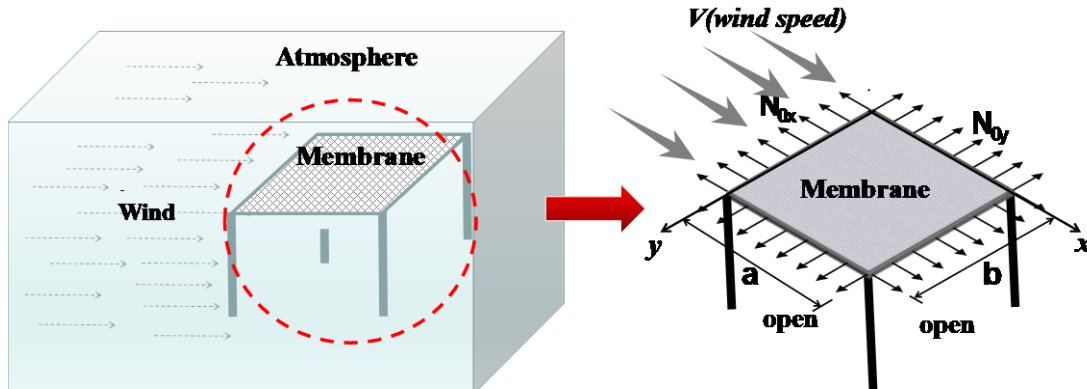
where f is the vibration amplitude corresponding to the instability critical wind speed. It shows that the critical wind speed is related to the vibration amplitude. Considering the influence of geometric nonlinearity of membrane, the stiffness of membrane will change with the change of amplitude in the process of vibration, which will affect the aerodynamic stability of membrane roof to a certain extent, which is consistent with the conclusions of previous research. When $f \rightarrow 0$, the critical wind speed of instability can be obtained according to the theory of small deflection.

248

2.1.2. Solution of Flexible Membrane Roof on Open Structure

249

For membrane roofs open open structures, air flows from both sides of the membrane surface due to the smaller thickness of the membrane, which can be approximately determined by the thin-airfoil theory[]. The membrane roof on open structure is shown in Figure 2.



252

253

Figure 3. The membrane roof on open structure

254

255

For the membrane roof on open structure, the aerodynamic force acting on the unit area of the membrane projection surface is expressed as follows[7]:

256

257

$$p = \rho_0 \frac{\partial}{\partial t} \int_0^x \gamma_c(\xi, y, t) d\xi + \rho_0 V \gamma_c \quad (49)$$

Where γ_c is the density of vortices.

258

259

$$\gamma_c = aV\gamma_j = aV \left(a_{1j}T(t) + a_{2j} \frac{T'(t)}{V} \right), \quad (j = 1, 2, \dots, M \times N) \quad (50)$$

Substituting Equation (50) into Equation (9), yields:

260

261

$$(h \frac{\partial^2 \varphi}{\partial y^2} + N_{0x}) \frac{\partial^2 w}{\partial x^2} + (h \frac{\partial^2 \varphi}{\partial x^2} + N_{0y}) \frac{\partial^2 w}{\partial y^2} - 2\rho \xi_0 \frac{\partial w}{\partial t} + \rho_0 V \gamma_c + \rho_0 \int_0^y \frac{\partial \gamma_c}{\partial t} d\eta = \rho \frac{\partial^2 w}{\partial t^2} \quad (51)$$

262

Solutions of stress functions in compatible equations such as Equation (21), Substituting Equations (19) and (21) into Equation (51), yields:

263

264

$$\begin{aligned} \rho W \frac{d^2 T(t)}{dt^2} + 2\rho \xi_0 W \frac{dT(t)}{dt} - \left(N_{0x} \frac{\partial^2 W}{\partial x^2} + N_{0y} \frac{\partial^2 W}{\partial y^2} \right) T(t) \\ - h \left(\frac{\partial^2 \phi}{\partial y^2} \frac{\partial^2 W}{\partial x^2} + \frac{\partial^2 \phi}{\partial x^2} \frac{\partial^2 W}{\partial y^2} \right) T^3(t) - \rho_0 V \gamma_c - \rho_0 \int_0^y \frac{\partial \gamma_c}{\partial t} d\eta = 0 \end{aligned} \quad (52)$$

Using Bubnov-Galerkin method to integral Equation (52), yields:

265

266

$$\iint_S \left[\rho W \frac{d^2 T(t)}{dt^2} + 2\rho \xi_0 W \frac{dT(t)}{dt} - \left(N_{0x} \frac{\partial^2 W}{\partial x^2} + N_{0y} \frac{\partial^2 W}{\partial y^2} \right) T(t) \right. \\ \left. - h \left(\frac{\partial^2 \phi}{\partial y^2} \frac{\partial^2 W}{\partial x^2} + \frac{\partial^2 \phi}{\partial x^2} \frac{\partial^2 W}{\partial y^2} \right) T^3(t) - \rho_0 V \gamma_c - \rho_0 \int_0^y \frac{\partial \gamma_c}{\partial t} d\eta \right] W(x, y) dx dy = 0 \quad (53)$$

Where $S \in \{0 \leq x \leq a, 0 \leq y \leq b\}$.

267

Integrating Equation (53) and simplifying it, yields:

268

269

$$A \frac{d^2 T(t)}{dt^2} + B \frac{dT(t)}{dt} - CT(t) - DT^3(t) - E = 0 \quad (54)$$

Where:

270

271

272

273

274

275

276

277

278

279

280

281

282

283

284

285

286

287

288

289

290

291

292

293

294

295

296

297

298

299

300

301

302

303

304

305

306

307

308

309

310

311

312

313

314

315

316

317

318

319

320

321

322

323

324

325

326

327

328

329

330

331

332

333

334

335

336

337

338

339

340

341

342

343

344

345

346

347

348

349

350

351

352

353

354

355

356

357

358

359

360

361

362

363

364

365

366

367

368

369

370

371

372

373

374

375

376

377

378

379

380

381

382

383

384

385

386

387

388

389

390

391

392

393

394

395

396

397

398

399

400

401

402

403

404

405

406

407

408

409

410

411

412

413

414

415

416

417

418

419

420

421

422

423

424

425

426

427

428

429

430

431

432

433

434

435

436

437

438

439

440

441

442

443

444

445

446

447

448

449

450

451

452

453

454

455

456

457

458

459

460

461

462

463

464

465

466

467

468

469

470

471

472

473

474

475

476

477

478

479

480

481

482

483

484

485

486

487

488

489

490

491

492

493

494

495

496

497

498

499

500

501

502

503

504

505

506

507

508

509

510

511

512

513

514

515

516

517

518

519

520

521

522

523

524

525

526

527

528

529

530

531

532

533

534

535

536

537

538

539

540

541

542

543

544

545

546

547

548

$$278 \quad A_1 = A - \rho_0 a \iint_S \left(\int_0^y a_{2j} d\eta \right) W(x, y) dx dy$$

$$278 \quad B_1 = B - \rho_0 a V \iint_S \left(\int_0^y a_{1j} d\eta \right) W(x, y) dx dy - \rho_0 a V \iint_S a_{2j} W(x, y) dx dy$$

$$279 \quad C_1 = C + \rho_0 a V^2 \iint_S a_{1j} W(x, y) dx dy$$

280 The composition of equation (55) is consistent with the vibration control equation of
 281 closed membrane roof, and the solving process is consistent with the above, which is not
 282 discussed here. Thus, the expression of critical wind speed for single mode instability of open
 flexible membrane roof can be obtained as follows.

$$283 \quad V_{cr} = \pi \sqrt{\frac{m^2 b N_{0x} / 4a + n^2 a N_{0y} / 4b + 3h m^2 n^2 \pi^2 (\alpha + \beta) f^2 / 8ab}{\rho_0 a \frac{ab}{MN} \sum_{j=1}^{M \times N} a_{1j} \sin \frac{m\pi x_j}{a} \sin \frac{n\pi y_j}{b}}} \quad (56)$$

284 3. Analysis of the Effect of Geometric Nonlinearity on Critical Wind Speed

285 Assuming that the wind speed is in the X direction, $m = n = 1$, $b = 20m$, $N_{0x} = 2kN/m$,
 286 $N_{0y} = 2kN/m$. Next, the difference between the results of considering and not considering the
 287 geometrical nonlinearity of thin films is discussed, and the necessity of considering the
 288 geometrical nonlinearity of thin films in the design of such structures is given.

289 In this paper, the expression of critical wind speed derived from mathematics is related to
 290 the amplitude of membrane vibration. Because the geometric nonlinearity of membrane is
 291 considered, the stiffness of membrane will change with the change of amplitude in the process
 292 of vibration, which will affect the aerodynamic stability of membrane roof to a certain extent.

293 Definiting λ is the ratio of cross (Y) to along (X) wind direction span ratio. The variation
 294 of critical wind speed with vibration amplitude for two types of membrane roofs with different
 295 span ratios is shown in Figure 4.

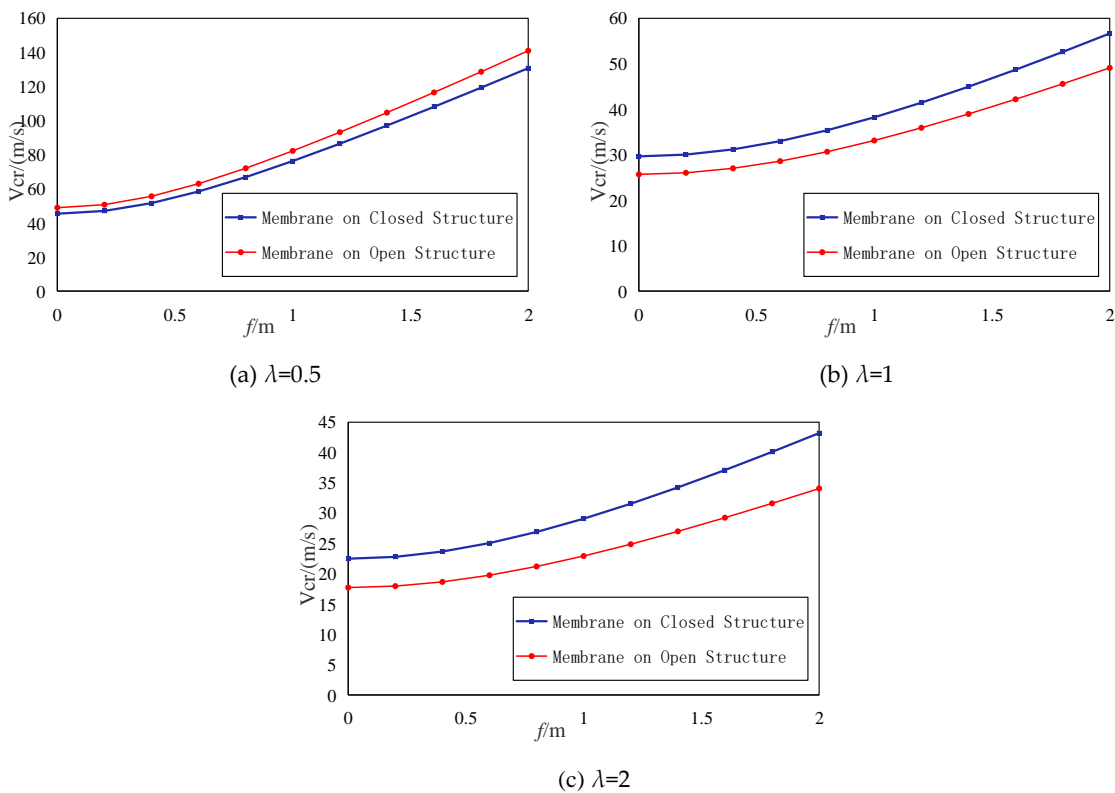


Figure 4. Curves of critical wind speed with amplitude for two types roof models

296
297
298
Taking membrane roof on closed structure as an example, considering the geometric
nonlinearity of membrane, the critical wind speed for single mode instability of closed
membrane roof is obtained by solving the equation.

299
300
$$V_{cr} = \sqrt{\frac{4\pi(m^2\pi^2b^2N_{0x} + n^2\pi^2a^2N_{0y}) + 3\varepsilon f^2(\rho\pi a^2b^2 + 4\rho_0 ab\alpha_1)}{8\pi b\rho_0 m\alpha_3}} \quad (57)$$

301
302
By substituting $f=0$ into Equation (57), the results of critical wind speed calculation without
considering geometric nonlinearity can be obtained.

303
304
$$V_{cr,L} = \pi \sqrt{\frac{a(m^2bN_{0x}/a + n^2aN_{0y}/b)}{2\rho_0 m\alpha_3}} \quad (58)$$

305
Comparing the critical wind speed of membrane roof on closed structure with and
without considering the geometric nonlinearity of membrane, the following results are
obtained:

306
$$\frac{V_{cr}}{V_{cr,L}} = \sqrt{1 + \frac{3\varepsilon f^2(\rho\pi a^2b^2 + 4\rho_0 ab\alpha_1)}{4\pi(m^2\pi^2b^2N_{0x} + n^2\pi^2a^2N_{0y})}} \quad (59)$$

307 4. Discussion

308
309
310
311
312
313
According to Equation (59), the critical wind speed of single mode instability obtained by
considering the geometrical nonlinearity of membrane is larger than the linear one. It shows
that the critical wind speed of instability obtained by neglecting the geometrical nonlinearity of
membrane is on the small side. It is conservative for structural design. By substituting the
specific values, the critical wind speed ratio $\frac{V_{cr}}{V_{cr,L}}$ of the membrane roof on closed structure can
be obtained as shown in Table 1.

314 Table 1. Critical wind speed ratio of membrane roof on closed structure with and without geometric
315 nonlinearity.

	$f=0.1m$	$f=0.2m$	$f=0.4m$	$f=0.6m$	$f=0.8m$	$f=1m$	$f=1.2m$	$f=1.4m$
$\lambda=0.5$	1.00	1.04	1.14	1.29	1.47	1.68	1.90	2.14
$\lambda=1$	1.00	1.01	1.05	1.11	1.19	1.29	1.40	1.52
$\lambda=2$	1.00	1.01	1.05	1.11	1.20	1.29	1.40	1.52

316
317
318
Similarly, the critical wind speed ratio $\frac{V_{cr}}{V_{cr,L}}$ of the membrane roof on open structure is
obtained as shown in Table 2.

319 Table 2. Critical wind speed ratio of membrane roof on open structure with and without geometric
320 nonlinearity.

	$f=0.1m$	$f=0.2m$	$f=0.4m$	$f=0.6m$	$f=0.8m$	$f=1m$	$f=1.2m$	$f=1.4m$
$\lambda=0.5$	1.00	1.04	1.14	1.29	1.47	1.68	1.90	2.14
$\lambda=1$	1.00	1.01	1.05	1.11	1.19	1.29	1.40	1.52
$\lambda=2$	1.00	1.01	1.05	1.11	1.20	1.29	1.40	1.52

321 From Table 1 and Table 2, it can be seen that when the cross-wind span ratio is small, the
322 geometric nonlinearity has a greater impact on the critical wind speed of single-mode
323 instability of membrane roof, and increases with the increase of vibration amplitude. When the
324 span ratio is greater than 1, the effect is relatively small. Article 5.3.4 of China's Technical
325 Regulations for Membrane Structures (CECS 158:2015)[12] stipulates that for integral tensioned
326 and cable-supported membrane structures, the deformation of the membrane structure should
327 not be greater than 1/200 of the span when considering the combination of wind load effects. In
328 this example, the normal displacement is limited to 0.1m, and the critical wind speed ratio is
329 1.00 when geometric nonlinearity is considered or not. Therefore, under normal wind loads,
330 the influence of membrane geometric nonlinearity on the aerodynamic stability of roofs can be
331 neglected. However, under strong wind loads, the deformation of roofs will exceed the norm
332 limit. At this time, the influence of geometric nonlinearity should be considered.

333 5. Conclusions

334 In this paper, the aerodynamic stability of orthotropic rectangular planar membranes on closed
335 and open structures is studied by mathematical analytic method. The governing equations of
336 wind-induced nonlinear vibration of tensioned membrane roofs are established by using the theory
337 of large deflection of membrane and Darumbell's principle. According to Bubnov-Galerkin method,
338 the governing equations of aerodynamic coupling are transformed into second-order non-linear
339 differential equations with constant coefficients and their periodic solutions are obtained by using
340 the improved multi-scale method. By judging the stability of the periodic solutions of the equations,
341 critical wind speed for single mode instability of the membrane roof considering geometric
342 nonlinearity is obtained. The influence of geometrical nonlinearity on the critical wind speed of
343 single-mode aeroelastic instability of membrane material is quantitatively obtained by comparing
344 the results with those without consideration. The main conclusions can be summarized as follows:

345 Considering the geometric nonlinearity of membrane vibration, the critical wind speed of
346 single mode instability of membrane roof increases nonlinearly with the increase of transverse
347 vibration displacement of membrane.

348 The critical wind speed of single mode instability with the geometrical nonlinearity of
349 membrane considered is larger than that of linear results. It shows that the critical wind speed of
350 membrane is small when the geometrical nonlinearity of membrane is neglected. For structural
351 design, it is conservative. When the span along the wind direction is small, the geometrical
352 nonlinearity has a great influence on the critical wind speed of single mode instability of membrane
353 roof, and with the amplitude of vibration. When the span ratio is greater than 1, the influence is
354 relatively small.

355 Under normal wind loads, the influence of membrane geometric nonlinearity on the
356 aerodynamic stability of roofs can be neglected. However, under strong wind loads, the
357 deformation of roofs may exceed the norm limit and reach about 3% of the span, the influence of
358 geometric nonlinearity should be considered.

359 **Author Contributions:** All authors contributed equally in writing this article. All authors read and approved
360 the final manuscript.

361 **Funding:** This research was funded by the National Natural Science Foundation of China (Grant No. 51608060)
362 and the Scientific and Technological Research Program of Chongqing Municipal Education Commission (Grant
363 No. KJ1723378).

364 **Acknowledgments:** In this section you can acknowledge any support given which is not covered by the author
365 contribution or funding sections. This may include administrative and technical support, or donations in kind
366 (e.g., materials used for experiments).

367 **Conflicts of Interest:** The authors declare no conflict of interest.

369 **References**

370

371 1. C.H. Jenkins, J.W. Leonard, Nonlinear dynamic response of membranes: state of the art, *Applied Mechanics*
372 *Reviews* 1996, 49, pp. 41–48.

373 2. Y., Wu; X.Y., Sun; S.Z., Shen. Computation of wind-structure interaction on tension structures. *Journal of*
374 *Wind Engineering & Industrial Aerodynamics* 2008 , 96, PP. 2019-2032.

375 3. A, Miyake; T, Yoshimura; M, Makin. Aerodynamic instability of suspended roof models. *Journal of Wind*
376 *Engineering and Industrial Aerodynamics* 1992, 42, PP. 1471-1482.

377 4. Y., Wu; S.Z., Shen. Research Progress on Fluid-Solid Interaction Effect of Wind-Induced Vibration
378 Response of Membrane Structure. *Journal of Architecture and Civil Engineering* 2006, 23, pp. 1-9.

379 5. Q.S., Yang; R.X.; Liu. On Aerodynamic Stability of Membrane Structures. *Engineering Mechanics* 2006, 23,
380 pp. 18-24.

381 6. R.X.; Liu; Q.S., Yang. The Wind-Structure Interaction Equation of Membrane Roofs With Small Sag.
382 *Engineering Mechanics* 2004, 21, pp. 41-44.

383 7. Xu, Y.P.; Zheng, Z.L.; Liu, C.J.; Song, W.J.. Aerodynamic Stability Analysis of Geometrically Nonlinear
384 Orthotropic Membrane Structure with Hyperbolic Paraboloid. *Journal of Engineering Mechanics*, 2011 , 137 ,
385 PP. 759-768.

386 8. Z.L.,Zheng; Y.P., Xu; C.J.,Liu. Nonlinear aerodynamic stability analysis of orthotropic membrane
387 structures with large amplitude. *Structural Engineering & Mechanics*, 2011, 37, pp. 1-4.

388 9. C.J.,Liu, X, Deng, Z.L.,Zheng. Nonlinear wind-induced aerodynamic stability of orthotropic saddle
389 membrane structures. *Journal of Wind Engineering and Industrial Aerodynamics*. 2017, 164, pp. 119-127.

390 10. Z.L., Zheng; W.J., Song. Study on Dynamic Response of Rectangular Orthotropic Membranes under
391 Impact Loading. *Journal of Adhesion Science and Technology*. 2012, 26, pp. 1467-1479.

392 11. Z.Q., Chen; Y., Wu; X.Y., Sun. Research on aeroelastic instability mechanism of closed-type one-way
393 tensioned membrane. *Journal of Building Structures*. 2015, 36, pp.12-19.

394 12. China Association for Engineering Construction Standardization. Technical specification for membrane
395 structures, China Planning Press, China, 2015; pp. 15-18.

396 13. Micallef K; Fallah, A.S.; Curtis, P.T.. On the dynamic plastic response of steel membranes subjected
397 to localised blast loading. *International Journal of Impact Engineering* 2015, 89, pp. 25-37.

398 14. Babu, A.A.; Sudhagar, P.E.; Rajamohan, V.. Dynamic characterization of thickness tapered laminated
399 composite plates. *Journal of Vibration and Control*.2016, 22, pp. 3555-3575.

400 15. Balkan, D.; Mecitoglu, Z.. Nonlinear dynamic behavior of viscoelastic sandwich composite plates under
401 nonuniform blast load: theory and experiment. *International Journal of Impact Engineering* 2014, 72, pp.
402 85-104.

403 16. D., L; Z.L., Zheng; et al.. Analytical Solutions for Stochastic Vibration of Orthotropic Membrane under
404 Random Impact Load. *Materials*, 2018, 11, pp. 1231-1259.

405 17. Y.Y., Zhang; Q.L., Zhang; et al.. Load-dependent mechanical of membrane materials and its effect on the
406 static behaviors of membrane structures, *Journal of Materials in Civil Engineering*, 2015, 51, pp. 468–473.